Shape-persistent macrocycles comprising perfluorinated benzene subunits: synthesis, aggregation behaviour and unexpected μ-rod formation†

Lijin Shu,[a] Marcel Müri,[b] Ralph Krupke[a] and Marcel Mayor*[a,b]

Received 2nd October 2008, Accepted 24th December 2008
First published as an Advance Article on the web 5th February 2009
DOI: 10.1039/b817274a

The synthesis of a series of shape-persistent macrocycles (SPMs) (**1–4** and **6**) comprising different numbers and/or spatial arrangement of *meta*-substituted tetrafluorobenzene and benzene subunits interlinked with diacetylenes is described. To increase their solubility, all five SPMs were functionalized by four peripheral hexyl chains. These SPMs were assembled from common diacetylene building blocks by a modular synthetic strategy based on palladium and/or copper catalyzed versions of acetylene coupling reactions (oxidative acetylene coupling and *Cadiot–Chodkiewicz* coupling). The aggregation properties in chloroform of SPMs **1–6** were investigated by concentration- and temperature-dependent ^{1}H-NMR investigations and by vapour pressure osmometry studies. Aggregation constants and thermodynamic data of the process were obtained by least-squares fitting of the NMR data and by *van't Hoff* analysis respectively. Aggregation was only observed for SPMs **2–6** comprising electron deficient tetrafluorobenzene corner units. While dimerization was the major aggregation process for SPMs **3–6**, the formation of larger aggregates in solution was only observed for SPM **2**. The formation of aggregates is in all cases enthalpically driven. As the largest and the smallest enthalpic contribution and entropic loss in the series of aggregating SPMs were found for the two SPMs **3** and **4**, each comprising two fluorinated corner units, the spatial arrangement of these subunits within the macrocycle seems to be at least equally important as the ratio of tetrafluorobenzene and benzene moieties. Interestingly, micro-scaled hexagonal rods were formed from SPM **3** upon heating in toluene, presumably consisting of mixtures of oligomers arising from covalently interlinked macrocycles.

Introduction

Shape-persistent macrocycles (SPMs) gained considerable attention during the last decade.[1–7] As rigid nanoscale scaffolds they are not only able to control the intramolecular spatial arrangement of functional groups and subunits,[3,8–15] but also to organize their intermolecular self-assembly in solution[2,6,7,16–19] and on 2D substrates.[8,20,21] Furthermore, their aggregation properties make them promising building blocks for nanoscale objects[22,23] and tailor-made functional materials.[4,18,24,25] Since Moore and co-workers reported the dimer formation of SPMs due to π–π stacking,[26,27] numerous new SPM model compounds were synthesized to investigate the phenomenon in detail. In particular, SPMs comprising electron-donating[28] and electron-withdrawing[14,19] substituents,[26,27,29] hydrogen bonding units,[30] and chiral building blocks[31,32] were synthesized to examine their aggregation properties. First theoretical models to calculate assembling properties of SPMs have been reported.[33]

We recently reported the synthesis of the SPM **5** consisting of diyne linked alternating hexylbenzene and tetrafluorobenzene subunits displaying an increased dimerization tendency arising from quadrupole interactions between the electron rich and electron poor subunits of the formed dimer.[19] The considerable π–π stacking interactions between fluorinated benzene and benzene were first reported by Patrick and Prosser in 1960.[34] Since then, the phenomenon has been investigated in detail[35] with designed model compounds including either intramolecular[36,37] or intermolecular[38–41] π–π stacking interactions.[42,43] In addition, theoretical models provide further insight into the nature of the intermolecular interactions.[33,44] Meanwhile, the supramolecular synthon has been applied successfully in crystal engineering,[45–58] surface patterning,[59] topochemistry[60,61] and to preorganize reactants.[62–64] Furthermore, fluorinated benzene subunits have been incorporated to tune material properties of liquid crystals,[65–67] polymers,[68,69] hydrogels,[70] adjustable networks,[71] optically active materials[72–74] and even biomolecules[75] like DNA[76,77] or peptides.[78]

Aggregation properties of macrocycles incorporating *meta*-ethynyl or -diyne interlinked benzene corner units have already been investigated. Increased aggregation tendencies were observed for SPMs comprising electron deficient benzene subunits and, thus, benzoate based subunits with their electron-withdrawing *exo*-annular substituents were used as aggregation favouring corner units.[26,29] In addition, a strong solvent dependence of the aggregation behaviour was observed.[79] The objective of this study is to investigate the potential of tetrafluoro-substituted benzene

[a]*Forschungzentrum Karlsruhe GmbH, Institute for Nanotechnology, P. O. Box 3640, D-76021 Karlsruhe, Germany. E-mail: marcel.mayor@kit.edu; Fax: +49 7247 82 5685; Tel: +49 7247 82 6392*
[b]*University of Basel, Department of Chemistry, St. Johannsring 19, CH-4056 Basel, Switzerland. E-mail: marcel.mayor@unibas.ch; Fax: +41 61 267 1016; Tel: +41 61 267 1006*

† Electronic supplementary information (ESI) available: Tables of the temperature and concentration dependent ^{1}H-NMR investigations, describtion of the solubility studies and the tables of the data displayed in Fig. 2 and 3. See DOI: 10.1039/b817274a

corners as aggregation-steering subunits. Thus, the macrocycles **1–6** were synthesized and characterized as a family of SPMs comprising different numbers and/or different spatial arrangement of perfluorinated subunits (Fig. 1). Their aggregation and dimerization was investigated in chloroform by concentration dependent ^{1}H-NMR experiments and by vapour pressure osmometry studies. Aggregation constants K were determined at various temperatures, providing further insights into the thermodynamic driving forces of the aggregation process.

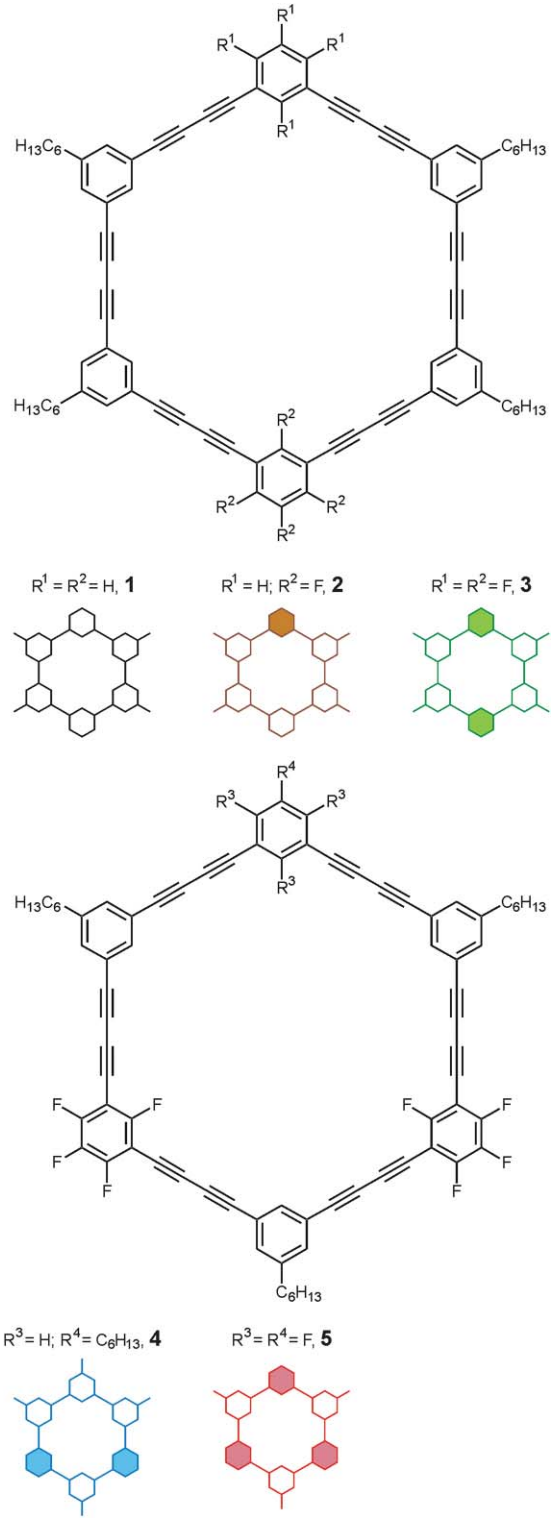

Fig. 1 Chemical structures and schematic representation of the SPMs **1–5**. White hexagons represent a benzene subunit while coloured hexagons represent a tetrafluorobenzene subunit.

Results and discussion

Synthesis

All five SPMs **1–5** consist of six aromatic corner units interlinked with diacetylenes in the *meta*-position. To increase the solubility of these structures in organic solvents, particular benzene subunits are functionalized with additional hexyl chains in the remaining *meta*-positions. To keep the series of macrocycles as comparable as possible, with the obvious exception of **5**, each cycle is functionalized with four alkyl chains. The diacetylene linker allows for a modular assembly of the SPMs from suitable *meta*-diyne-functionalized benzene building blocks. Symmetric diacetylenes can be obtained by a *Glaser*-type oxidative acetylene coupling reaction[80,81] while for asymmetric acetylenes both precursors are distinguished as acetylene and bromoacetylene allowing for a *Cadiot–Chodkiewicz* coupling reaction.[81,82]

The assembly of the SPMs **1–4** is displayed in Scheme 1, while the synthesis of the SPM **5** with periodically alternating tetrafluorobenzene and hexylbenzene subunits has already been reported.[19] First, the differently functionalized 1,3-diethynylbenzene building blocks **8–12** were synthesized. 1,3-Bis(bromoethynyl)benzene (**8**) was obtained by brominating the commercially available 1,3-diethynylbenzene (**7**). The diyne **7** was treated with *N*-bromosuccinimide (NBS) and traces of $AgNO_3$ in acetone to provide the desired dibromoacetylene **8** in 77% yield after purification by column chromatography (CC). By applying similar reaction conditions, 1,3-bis(bromoethynyl)-5-hexylbenzene **10** was obtained as a slightly yellowish oil in 91% yield from 1,3-diethynyl-5-hexylbenzene (**9**). The diyne **9** and the mono protected diyne **11** were obtained in four steps following a published protocol.[19] These precursor syntheses start with 4-hexylaniline which is doubly brominated to 2,6-dibromo-4-hexylaniline. Deamination followed by substitution of both bromines with triisopropylsilyl (TIPS) protected acetylenes in a *Sonogashira*-type[83,84] coupling reaction provided the doubly protected diyne precursor. Gentle deprotection gave a mixture of the doubly deprotected diyne **9** and the mono protected diyne **11** which were isolated by CC. The synthesis of the 1,2,3,5-tetrafluoro-4,6-bis(bromoethynyl)benzene building block **12** was reported elsewhere.[19] Tetrafluoroisophthalonitrile was reduced to tetrafluoroisophthalaldehyde and a *Corey–Fuchs* reaction sequence[85] provided the dibromoacetylene precursor **12**.

With the required precursors **7–12** in hand, the stepwise assembly of the SPMs was undertaken. The semicycles **13**, **16** and **18**, comprising terminal TIPS protected acetylenes, were obtained by a palladium and copper catalyzed variation of the *Cadiot–Chodkiewicz* coupling reaction.[86] Thus, the dibromoacetylene precursors **8**, **10** and **12** were treated with two equivalents of the mono protected diyne **11** in the presence of $Pd_2(dba)_3{\cdot}CHCl_3$ and CuI as catalysts to provide the doubly TIPS protected semicycles **13**, **16** and **18** in 66%, 24% and 67% yields respectively after CC. The corresponding free acetylenes **14**, **17** and **19** were obtained by treating the TIPS protected precursors with TBAF in wet

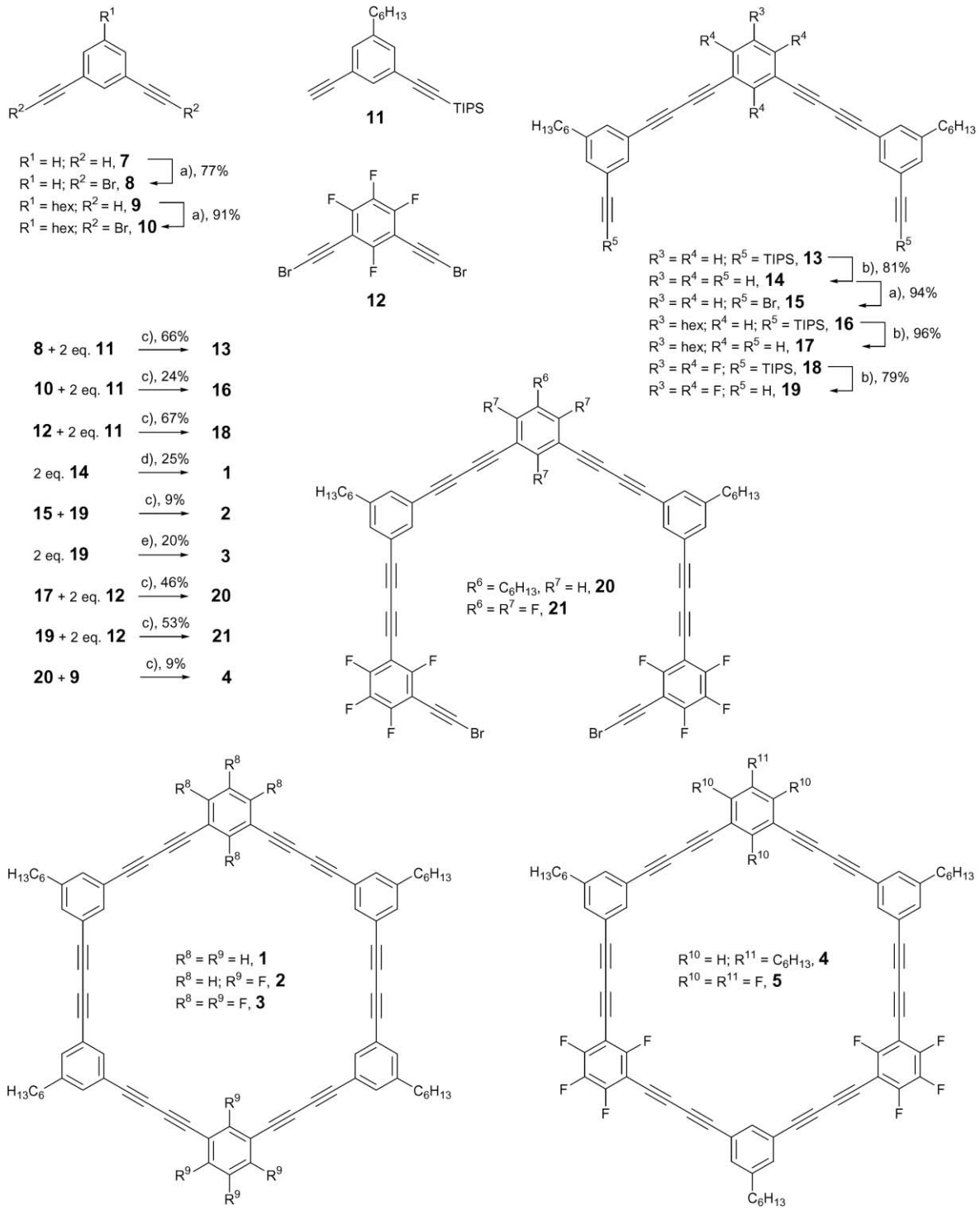

Scheme 1 Synthesis of the SPMs **1–4** and their precursors. *Reagents and conditions*: a) NBS, $AgNO_3$, CH_3COCH_3, r.t.; b) TBAF, wet THF, r.t.; c) $Pd_2(dba)_3{\cdot}CHCl_3$, CuI, $C_6H_5CH_3$, $EtN(i\text{-}Pr)_2$, r.t.; d) $Cu(CH_3CO_2)_2{\cdot}H_2O$, C_5H_5N, C_6H_6, r.t.; e) $PdCl_2(PPh_3)_2$, CuI, THF, $EtN(i\text{-}Pr)_2$.

THF at room temperature. Thus the diacetylenes **14**, **17** and **19** were obtained in 81%, 96% and 79% yields respectively after CC. The semicycle **15** comprising two terminal bromoacetylenes was isolated by CC in 94% after treating the diyne semicycle **14** with NBS and traces of $AgNO_3$.

Using these semicycles, the macrocycles **1**, **2** and **3** were assembled. For the SPM **1** a pseudo high dilution variation of an oxidative acetylene coupling was applied. A suspension of $Cu(CH_3CO_2)_2{\cdot}H_2O$ in 300 mL pyridine and 200 mL benzene was stirred vigorously under air while a solution of the semicyclic diacetylene **14** dissolved in 100 mL benzene was added dropwise over a period of 24 hours at room temperature. After stirring the reaction mixture at room temperature for another 2 days, the solvents were evaporated and the residue redissolved in

toluene. Filtration and subsequent separation by size exclusion chromatography (SEC) provided the macrocycle **1** in 25% yield as a brown solid. Most likely, the formation of larger open chain and cyclic oligomers under the applied reaction conditions are responsible for the moderate yield of isolated SPM **1**. These side products of larger molecular weight were not further investigated.

For the assembly of the macrocycle **2**, a pseudo high dilution variation of the above-described Pd and Cu catalyzed version of the *Cadiot–Chodkiewicz* coupling reaction was applied. To a nitrogen purged mixture of 450 mL toluene and 5 mL diisopropylethylamine containing $Pd_2(dba)_3{\cdot}CHCl_3$ and CuI as catalysts, a solution of equimolar amounts of the semicycles **15** and **19** in 40 mL toluene was added dropwise over a period of 10 hours at room temperature. The reaction mixture was allowed to stir at room temperature for another 4 days. The solvents were removed and the remaining residue redissolved in 15 mL toluene. After filtration and SEC, the macrocycle **2** was obtained in 9% yield as a light brown solid. Also in this case, the expected side products of larger molecular weights were not further investigated.

To assemble the macrocycle **3**, comparable pseudo high dilution conditions were applied for a Pd and Cu catalyzed variation of the oxidative acetylene coupling.[87] Thus, a mixture of 15 mL diisopropylethylamine in 1.2 L dry THF containing $PdCl_2(PPh_3)_2$ and CuI as catalyst and dry silica gel as a water trap was stirred under dry air. A solution of the semicycle **19** in 100 mL dry THF was added dropwise over a period of 10 hours. The reaction mixture was stirred for another 4 days before the solvents were removed and the remaining residue was dissolved in 15 mL toluene. Filtration through a short plug of silica gel and separation by SEC provided the SPM **3** in 20% yield as a brown solid. The oligomeric side products were not further investigated.

In contrast to the SPMs **1–3**, the macrocycle **4** was not assembled from two hemicycles but by a stepwise elongation of the semicycle **17**. Thus, the diyne **17** was treated under the Pd and Cu catalyzed reaction conditions already described above with an excess of the bromoethynyl-functionalized tetrafluorobenzene building block **12**. In order to maximize the relative concentration of the bromoacetylene precursor **12** with respect to the diyne **17**, 7.7 equivalents of **12** were dissolved together with the catalysts in a degassed diisopropylethylamine/toluene mixture to which a solution of the diyne **17**, dissolved in toluene, was added dropwise over a period of 2% hours at room temperature. After stirring for additional 2 hours, removal of the solvents and purification by CC, the terminal bromoethynyl-functionalized pentamer **20** was isolated in 46% yield as a yellow solid. To close the cycle **4**, its precursors **20** and **9** were treated under comparable high dilution conditions as described above for the synthesis of SPM **2**. Thus, to a vigorously stirred and degassed mixture of the catalysts $Pd_2(dba)_3{\cdot}CHCl_3$ and CuI dissolved in 450 mL toluene and 5 mL diisopropylethylamine a solution comprising equimolar amounts of the dibromoacetylene **20** and the diacetylene **9** dissolved in 40 mL toluene was added dropwise over 10 hours at room temperature. After stirring for 4 days, the solvents were removed and the residue redissolved in toluene. Filtration and purification by SEC provided the SPM **4** in 9% yield as a brown solid. A considerable fraction of the crude reaction products passed faster through the SEC column than the SPM **4** suggesting the presence of higher molecular weight oligomers which were not further investigated.

The successful ring closure between the doubly bromoacetylene-functionalized pentamer **20** and the diyne **9** to the SPM **4** led us to investigate similar reaction conditions with the diyne **19** and the dibromoacetylene **21** to obtain the enlarged macrocycle **6** consisting of eight aromatic corner units (displayed in Scheme 2). In analogy to the SPM **5**, the highly symmetric macrocycle **6** consists of alternating tetrafluorobenzene and hexylbenzene subunits. However, the expansion of the ring no longer allows for planarity of the cyclic system which might be reflected in its association behaviour. Applying comparable reaction conditions to the precursors **19** and **21** as for **9** and **20** during the synthesis of **4**, the macrocycle **6** was isolated in an even lower yield of 6% as a white solid after SEC.

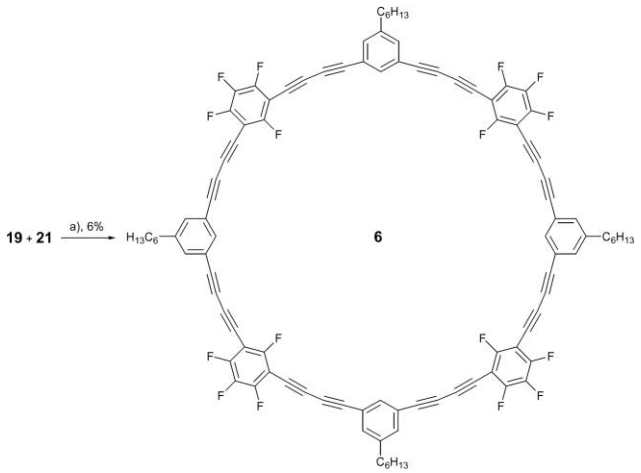

Scheme 2 Synthesis of the macrocycle **6**. *Reagents and conditions*: a) $Pd_2(dba)_3{\cdot}CHCl_3$, CuI, $C_6H_5CH_3$, $EtN(i\text{-}Pr)_2$, r.t.

The macrocycles **1–6** and their precursors were fully characterized by ^{1}H-, ^{13}C- and ^{19}F-NMR spectroscopy, mass spectrometry and elemental analysis. However, the limitations in solubility and availability of the macrocycle **2** combined with its rather low symmetry and the multiple splitting of the carbon signals of perfluorinated benzenes, did not allow to resolve the aromatic carbons of its tetrafluorobenzene subunit in the ^{13}C-NMR spectrum.

Stacking investigations

^{1}H-NMR investigations. Due to the limited solubility of these SPMs in polar solvents such as acetonitrile or methanol, their aggregation properties were investigated exclusively in chloroform. Thus, their ^{1}H-NMR spectra were recorded in $CDCl_3$ at various concentrations and temperatures. However, the observable concentration windows were limited by the solubilities of these SPMs in chloroform. In particular, the saturation-concentrations at 25 °C in chloroform of the macrocycles **1**, **2**, **3** and **6** were 2.75 mmol/L, 5.15 mmol/L, 1.96 mmol/L and 2.64 mmol/L respectively. Interestingly, the SPM **4** displayed the highest saturation-concentration (31 mmol/L). Only the SPM **5** (25 mmol/L) was comparable.

Within the observable concentration window (0.5–2.75 mmol/L) the chemical shifts of both, the *exo*- and the *endo*-annular protons of SPM **1** were concentration independent. This concentration independent behaviour points at dissolved monomeric molecular species in this concentration regime, as previously

reported for comparable SPMs like *e.g.* phenyl ethynyl macrocycles peripherally functionalized with butylcarboxylates, butylether- or benzylbutylether-groups.[2]

In contrast to **1**, the chemical shifts of the proton signals of the SPMs **2–6** depended on their concentrations. For all five SPMs the *exo*-annular protons displayed a stronger concentration dependence (Fig. 2) than the *endo*-annular proton. Even in the narrow concentration range required to observe a detectable ^{1}H-NMR signal and the solubility of the SPM in $CDCl_3$ at 10 °C, a considerable shift towards higher field with increasing concentration was observed, suggesting intermolecular π–π stacking. As expected, the presence of both corner units, benzene and tetrafluorobenzene is required to promote π–π stacking by quadrupole interactions in the investigated solvent, temperature and concentration regimes. While the chemical shift *vs.* concentration slopes (Fig. 2) of the SPMs **4** and **5** allow to anticipate an asymptotic approach towards a signal for infinite concentration, this was not the case for the SPMs **2**, **3** and **6** due to their limited concentration window. However, the slopes of **3** and **6** resemble strongly the more pronounced concentration dependent initial branch of the slopes of **4** and **5** and thus, it seems likely that the asymptotic branch is cut off due to the solubility restrictions. A less pronounced upfield shift with increasing concentration was observed for SPM **2**.

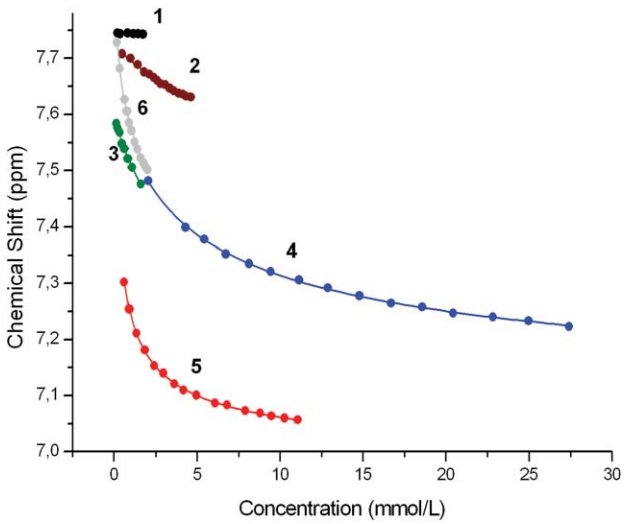

Fig. 2 Concentration dependence of the ^{1}H-NMR chemical shifts of the *exo*-annular protons of the macrocycles **1–6** in $CDCl_3$ at 10 °C. The dots are the measured values and the solid lines are the fitted titration curves.

These ^{1}H-NMR investigations, displaying systematic changes of the chemical surrounding of the macrocycles comprising tetrafluorobenzene subunits with concentration, strongly point at intermolecular stacking events. However, the number of SPMs involved in the formation of these stacked supermolecules cannot be determined by these titration experiments.

Vapour pressure osmometry (VPO). The stacking behaviour of the SPMs **1–4** and **6** was further investigated by VPO to inspect whether the chemical shifts observed in the ^{1}H-NMR studies arise from dimerization of these SPMs or from the formation of larger oligomeric piles consisting of several stacked SPMs. Thus, the averaged molecular weights of dissolved species were measured for these SPMs at various concentrations which are listed in Table 1.

Very comparable molecular weights were obtained at all four concentrations of SPM **1** in $CHCl_3$ at 37 °C. The values between 1302 and 1090 g/mol are comparable with the molecular weight (1081 g/mol). This suggests the presence of freely dissolved SPMs without intermolecular stacking, as observed by ^{1}H-NMR studies. It is noteworthy that several of the SPM solutions listed in Table 1 are clearly below the critical lower concentration of about 2 mmol/L (~0.003 mol/kg) suggested for the VPO apparatus (Knauer VPO K-7000) and thus, these data should be considered as semi-quantitative, diagnostic for stacking interactions.

Due to the poor yield in its synthesis, only very limited amounts of the SPM **2** comprising a single tetrafluorobenzene subunit were available for VPO investigations. Thus, only two concentrations were measured to study its stacking behaviour. A 0.82 mmolar solution of SPM **2** in $CHCl_3$ at 37 °C displayed a value (1139 g/mol) corresponding to the SPM molecular weight (1153 g/mol), pointing at completely dissolved individual molecules **2** at this concentration. More surprising was the value of 3780 g/mol at a concentration of 3.38 mmol/L which suggests the presence of at least trimeric stacked species under the investigated conditions. As the majority of SPMs reported so far were either not aggregating or forming only dimers, the observation of larger oligomers by VPO for SPM **2** was unexpected. Unfortunately, the available quantity of SPM **2** did not allow investigation of its stacking behaviour in further detail.

Table 1 Concentration dependent average molecular weight of the aggregates formed by the macrocycles **1–4** and **6** in $CHCl_3$

1[a]		**2**[a]		**3**[b]		**4**[b]		**6**[a]	
$C_{84}H_{72}$		$C_{84}H_{68}F_4$		$C_{84}H_{64}F_8$		$C_{84}H_{64}F_8$		$C_{104}H_{64}F_{16}$	
1081.47 g/mol		1153.43 g/mol		1225.39 g/mol		1225.39 g/mol		1617.60 g/mol	
conc. (mmol/L)	mwt. (g/mol)	conc. (mmol/L)	mwt. (g/mol)	conc. (mmol/L)	mwt. (g/mol)	conc. (mmol/L)	mwt. (g/mol)	conc. (mmol/L)	mwt. (g/mol)
0.31	1302	0.82	1139	0.57	623	0.82	1136	0.32	1609
1.2	1120	3.38	3780	1.14	1022	1.22	2169	0.87	2411
2.31	1124			2.28	1619	2.69	2247		
4.99	1090			4.65	1930	5.63	2012		
				9.46	2133	10.85	2254		

[a] Measured at 37 °C. [b] Measured at 42 °C.

The SPM **3**, comprising two tetrafluorobenzene subunits facing each other on the cycle's periphery (1,4-position), was available in larger amounts. To expand the scope of addressable concentrations, the solvation of **3** in $CHCl_3$ at 42 °C was assisted by ultrasonic sonication. A maximum concentration of 9.46 mmol/L was reached as a slightly cloudy solution without observable precipitation. As displayed in Table 1, an increase of the average molecular weight of the dissolved species with concentration was observed for SPM **3**. However, even at the maximum concentration a molecular weight (2133 g/mol) below the one expected for complete dimer formation (2450 g/mol) was recorded. Thus, the dominant assembly process of SPM **3** is most likely dimeric.

The SPM **4** comprises, as SPM **3**, two tetrafluorobenzene subunits, but in 1,3-positions with respect to the corner units of the SPM. Intrestingly, this structural variation makes the SPM about ten times more soluble. Again, its aggregation in $CHCl_3$ at 42 °C was investigated by VPO. As displayed by the data in Table 1, the VPO investigations do not really benefit from the increased solubility of **4**. While a molecular weight of 1136 g/mol pointing to a monomeric dissolved species (1225 g/mol) was observed at a concentration of 0.82 mmol/L, all investigated concentrations above 1.22 mmol/L displayed values between 2012 g/mol and 2254 g/mol, pointing at stacked dimers of SPM **4**. Again, dimer formation seems to be the dominant assembly process, as even for concentrations above 10 mmol/L, only values below the molecular weight of the dimer were observed.

VPO investigations of the SPM **6** were limited to only two concentrations due to the limited availability of the compound. SPM **6** is an expanded structural analog of SPM **5**, for which dimer formation has already been reported as the major assembly process in $CHCl_3$ at room temperature.[19] However, the expansion by two additional corner units reduces the planarity of **6** considerably and might influence its assembly behaviour. The values recorded in $CHCl_3$ at 37 °C displayed mainly the presence of dissolved monomeric species at a concentration of 0.32 mmol/L and its tendency to stack upon increasing the concentration to 0.87 mmol/L. The recorded average molecular weight does not point towards further aggregation beyond dimer formation. While the recorded VPO data and the similarity to SPM **5** point towards dimerization as the dominant aggregation process, the restricted amount of VPO data available for SPM **6**, combined with the limited accuracy of the method in the investigated concentration regime, hardly allows us to exclude the formation of larger stacks. Assuming dimer formation as the major aggregation behaviour, the average molecular weight of 2411 g/mol at a concentration of 0.87 mmol/L corresponds to about 50% of the molecules in solution aggregated as dimers.

In summary, the VPO studies pointed, in spite of the limited amounts of SPMs available and the borderline concentrations of the samples, towards dimerization as the major aggregation process for most of the studied SPMs. While the lack of aggregation was expected for SPM **1**, the tendency to form larger aggregates of SPM **2** was rather surprising. However, due to the limited availability of SPM **2**, this behaviour has been deduced from a single VPO solution which was reproduced in triplicate. All three measurements provided comparable results and the measured average molecular weight pointing at about trimeric species should be outside the variation and imperfection of the method and the apparatus. Thus, throughout the paper the formation of larger aggregates was considered exclusively for SPM **2**.

Association constants and thermodynamic data. The concentration dependent ^{1}H-NMR and VPO investigations allow determination of the association constants for the SPMs **2–4** and **6**. While the ^{1}H-NMR data are perfectly suited to extract the association constant by least-squares curve fitting, the VPO data are crucial to favour a particular association model for each SPM.[2] Thus, based on the osmometric data, a monomer–dimer equilibrium has been assumed as the major aggregation process of SPMs **3–6**. To obtain dimerization constants (K_{Dim}), eqn (1) with c_{tot} as the total concentration of the SPM and δ_{Mono} and δ_{Dim} as the chemical shifts of the monomer and the dimer respectively was used for least-squares curve fitting of the concentration dependent ^{1}H-NMR data.[88]

$$\delta = \delta_{Dim} + (\delta_{Mono} - \delta_{Dim}) \frac{\sqrt{8 \cdot K_{Dim} \cdot c_{tot} + 1} - 1}{4 \cdot K_{Dim} \cdot c_{tot}} \quad (1)$$

While the aggregation by dimerization of SPM **5** has already been reported,[19] the dimerization constants obtained by curve fitting at 20 °C are summarized in Table 2. Furthermore, the fitted curves at 10 °C are presented as solid lines in Fig. 2, displaying the good correlation between measured data points and calculated curves.

For the larger aggregates of SPM **2** an isodesmic association model was applied, assuming a general association constant independent from the extent of the already existing stack to which a monomer is aggregating ($K_{Dim} = K_3 = K_4 = \ldots\ldots = K_n = K_{Ass}$). To obtain association constants (K_{Ass}) of SPM **2**, least-squares curve fitting of the NMR data to eqn (2) was applied.[29,79] In eqn (2), δ is the chemical shift at the concentration of SPM **2** (c_{tot}), and δ_{Mono} and δ_{Ass} are the limiting chemical shifts of the monomer and the aggregate respectively.

$$\delta = \delta_{Ass} + (\delta_{Mono} - \delta_{Ass}) \frac{\sqrt{4 \cdot K_{Ass} \cdot c_{tot} + 1} - 1}{2 \cdot K_{Ass} \cdot c_{tot}} \quad (2)$$

The association constants obtained for SPM **2** are displayed together with the dimerization constants of the other SPMs at 20 °C in Table 2 and the fitted curve for 10 °C is displayed as a solid line in Fig. 2.

Furthermore, by varying the temperature of the concentration dependent ^{1}H-NMR investigations followed by least-squares curve fitting, association constants at different temperatures were obtained. The aggregation of each SPM was investigated at five different temperatures and a subsequent *van't Hoff* analysis

Table 2 Aggregation constants at 20 °C of SPMs **1–6** in $CDCl_3$ and thermodynamic data obtained by *van't Hoff* analysis

SPM	$K_{293\,K}$ (M^{-1})	$\Delta G_{293\,K}$ (kJ/mol)	$\Delta H_{293\,K}$ (kJ/mol)	ΔS (J/mol·K)
1[a]	~0			
2[b]	33.4 ± 21.2	−8.9 ± 4.0	−46.6 ± 2.0	−128.5 ± 6.8
3[c]	22.6 ± 12.1	−7.6 ± 4.8	−85.3 ± 4.4	−265.2 ± 16
4[c]	116.1 ± 19.2	−11.6 ± 2.7	−33.6 ± 1.3	−75.1 ± 4.6
5[c]	1875 ± 605	−18.3 ± 5.2	−64.1 ± 2.6	−156.3 ± 8.9
6[c]	176.2 ± 35.9	−12.6 ± 4.9	−63.9 ± 2.5	−172.9 ± 8.3

[a] No aggregation was observed in $CDCl_3$. [b] The formation of larger aggregates was observed by osmometry. [c] No larger aggregates than dimers were observed by osmometry.

provided thermodynamic data of the association process. Thus, plots of the natural logarithm of their association constants against the inverse absolute temperature should provide straight lines with $\Delta H/R$ as slopes and $-\Delta S/R$ as axis intercepts. In Fig. 3 the *van't Hoff* plots of the SPMs **2–6** are displayed and the extracted thermodynamic parameters of the association process are summarized in Table 2.

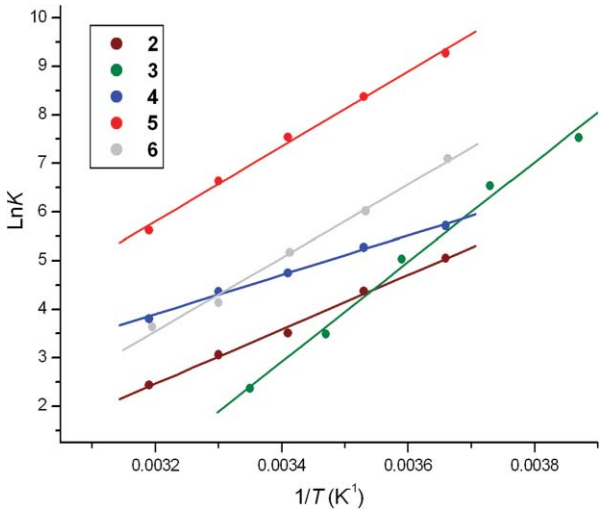

Fig. 3 *Van't Hoff* plots of the SPMs **2–6**. While for SPMs **3–6** the natural logarithm of the dimerization constant K_{Dim} was plotted, the natural logarithm of the association constant K_{Ass} obtained assuming an isodesmic association model was used for the SPM **2**. Least-squares fit of the data points provided the regression lines.

All five aggregating SPMs **2–6** have their enthalpically driven association with negative free energies at 20 °C ($\Delta G_{293\,K}$) in common. However, the enthalpic contributions to the associations of these different SPMs vary considerably, as can be seen by their different slopes in Fig. 3 or their enthalpies at 20 °C ($\Delta H_{293\,K}$) listed in Table 2. While both macrocycles **5** and **6** consisting of alternating hexylbenzene and tetrafluorobenzene corner units display comparable enthalpies at 20 °C, the largest and the lowest enthalpic contributions have both been observed by an SPM comprising two tetrafluorobenzene corner units, pointing at the crucial importance of the spatial arrangement of these subunits. The most negative enthalpy was observed for SPM **3**, having the two fluorinated corner units at opposite corners of the macrocycle (1,4-position) while the lowest enthalpic contribution was observed for SPM **4** with its two fluorinated corner units in the 1,3-position. The enlarged enthalpic stabilization of **3** compared with **5** was surprising at first glance, as the latter enables more stabilizing fluorobenzene/benzene couples in an aggregated dimer. However, the finding might be rationalized to some extent by the theoretically predicted rotational displacement (by 6.5°) of these fluorobenzene/benzene couples in an aggregated dimer.[33] While in a dimer of **5** the rotational displacement results to some extent in a reduced distance between repulsive fluorinated corner units, this is not the case for a dimer of SPM **3**. On the other hand, the weaker enthalpic contribution in the dimer of SPM **4** can be rationalized by (i) the lower number of stabilizing fluorobenzene/benzene couples compared with **5** and (ii) by the fact that for each possible dimer profiting from four stabilizing fluorobenzene/benzene interactions, a rotational displacement reduces the distance between repulsive fluorinated corner units.

Finally, the aggregation of SPM **2** displays a comparable weak enthalpic contribution as was observed for SPM **4**. However, while a rather low enthalpic contribution has been expected due to the low number of stabilizing interactions arising from a single fluorinated unit in the macrocycle, the comparison with the dimerizing SPMs is questionable to some extent due to its different aggregation mechanism.

The entropies (ΔS) listed in Table 2 oppose the trend observed for the enthalpic contributions of the dimerizing SPMs **3–6**. Namely, aggregation systems with a large enthalpic contribution have a large negative entropy. This is the expected observation that a strong aggregation tendency tends towards a more ordered system reflected in a large negative value for its entropy (ΔS). The number of solvent molecules released by aggregation is (i) not able to compensate the entropy loss by aggregation and (ii) assumed to be comparable for all investigated SPMs.

In addition, the aggregation constants at 20 °C are displayed in Table 2. As displayed by the various slopes in the *van't Hoff* plot, aggregation constants of these SPMs are strongly temperature dependent and the selection of 20 °C as the observation temperature is to some extent arbitrary. However, while the aggregation constants of SPMs **2–4** and **6** are all within one order of magnitude, the SPM **5** with a maximized number of stabilizing interactions and a favourable planar geometry displays a more than ten fold increased aggregation constant at 20 °C ($K_{293\,K}$(**5**) = 1875 ± 605 M^{-1}).

Temperature triggered formation of μ-rods

A surprising observation was made during the characterization of SPM **3**. Recording of the ^{13}C-NMR spectra of these macrocycles was challenging due to their limited solubility and the extensive coupling of carbon nuclei with peripheral fluorine substituents. Thus, ^{13}C-NMR spectra were recorded in d_8-toluene, which turned out to be able to dissolve considerable amounts of different fluorinated SPMs **2–6**. To further increase the amount of dissolved SPM **3**, the solution was heated to 50 °C. Initially, the increased temperature dissolved **3** completely in toluene. However, after a few hours, the compound precipitated again at this elevated temperature. Neither further increase of the temperature nor sonication of the sample allowed the formed precipitation to be redissolved.

Closer inspection of the precipitate by scanning electron microscopy (SEM) revealed well formed rod-like crystallites with a hexagonal cross-section as displayed in Fig. 4. The diameter of a typical crystallite is in the order of a few microns and its aspect ratio (length/diameter) is in the order of 10. Thus, these crystallites must consist of a large number of well ordered molecules.

Even more surprising than the self-assembly of these macrocycles at elevated temperature in well ordered crystallites was their behaviour during inspection by SEM. The as-prepared rods have numerous cracks perpendicular to their long axis (Fig. 4A) which disappear under progressive SEM imaging. As an example, Fig. 4B displays the same area of a crystallite as Fig. 4A after irradiation with the electron beam for about 5 minutes. This behaviour is very surprising for organic materials. Usually organic materials subjected to electron irradiation are unstable and tend to

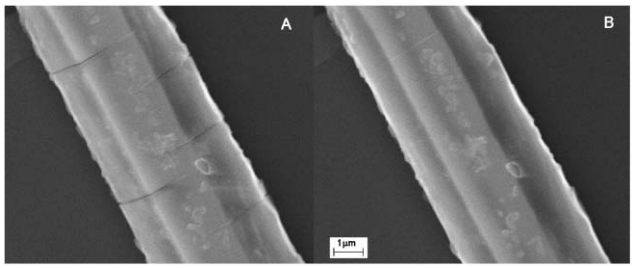

Fig. 4 SEM images of a hexagonal rod-like crystallite formed in a 50 °C hot solution of SPM **3** in toluene. As-prepared sample (A), after irradiation for 5 minutes (B).

charge up and disintegrate. Here the opposite is observed, namely defects in these crystallites are repaired under electron irradiation. Moreover, these crystallites do not show any sign of charging, pointing at an efficient charge transport mechanism in these µ-rods.

These observations show (i) that the 10 keV (1.6×10^{-15} J = 1.6 fJ) electrons provide sufficient energy to activate defect healing without causing significant structural damage and (ii) that charges can propagate through the material to the conducting substrate. The healing mechanism is observed on a micron length scale and thus, it is probably caused by an electron beam induced rearrangement of the molecular building blocks in the crystallite and not the result of a reaction on the molecular scale.

However, the fact that these crystallites are no longer soluble in hot toluene whereas freshly prepared samples of SPM **3** are raised the question concerning the molecular identity of the building blocks of these crystallites. Fortunately, after the screening of numerous solvents, dimethylformamide (DMF) turned out to be able to dissolve small amounts of these crystallites completely. Thus, a saturated toluene solution of SPM **3** was divided into two halves. While the first sample was evaporated to dryness, the second sample was heated to 50 °C for 48 hours and the thereby formed solution comprising considerable amounts of precipitated crystallites was evaporated to dryness. Subsequently, both samples were redissolved in equivalent amounts of DMF and investigated by gel permeation chromatography (GPC). While for the first sample mainly the signal of the SPM **3** was observed (Fig. 5A), the solution of these redissolved crystallites (Fig. 5B) displays signals of twice and three times the molecular weight of the macrocycle **3**, pointing at dimers and trimers.

Apparently, heating of a concentrated solution of SPM **3** in toluene provides covalently interlinked dimeric and trimeric structures. As a potential interlinking reaction an oligomerization of the diacetylene units of two stacked macrocycles was hypothesized. Similar reactions have already been reported triggered by light in the solid state for diacetylenes organized by supramolecular interactions of benzene and perfluorobenzene subunits.[62,89] Typical reaction products of diacetylene polymerizations contain but-1-en-3-yne subunits. Thus, the crystallites were further investigated by infrared spectroscopy, to search for new double bonds formed, pointing at these expected subunits. And indeed, the comparison of the IR spectra of the parent SPM **3** and the resulting crystallites (Fig. 6) displayed a new signal at $\lambda = 1695$ cm^{-1}, which can be assigned to a new carbon–carbon double bond in these crystallites. Unfortunately, further investigation by ^{13}C-NMR spectroscopy

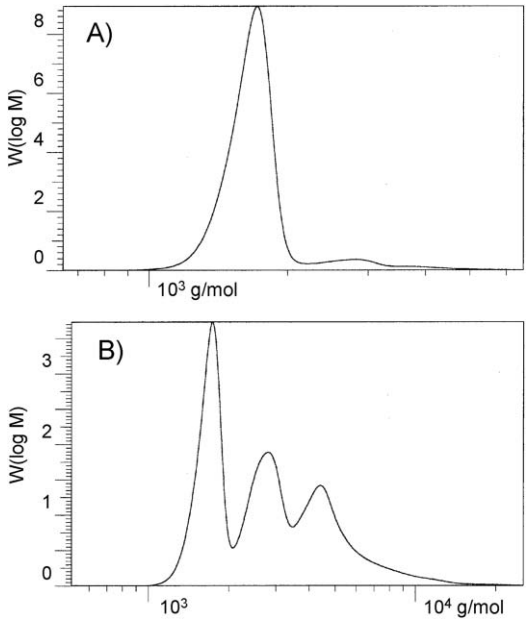

Fig. 5 GPC analysis of a solution of **3** in toluene (A) before and (B) after heating at 50 °C for 48 hours.

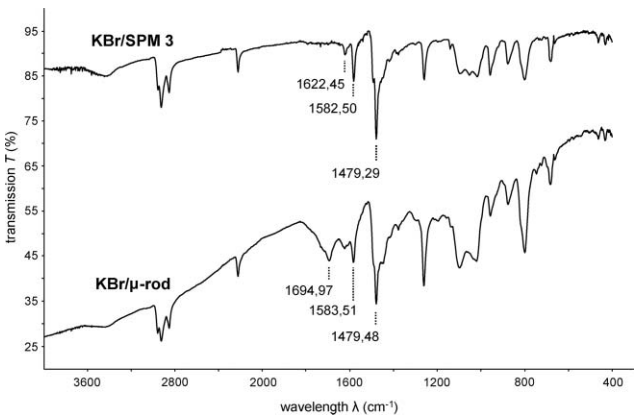

Fig. 6 Infrared spectra of the SPM **3** (top) and of the crystallites obtained from **3** upon heating in toluene (bottom). Both spectra were recorded as KBr pellets.

was not possible due to the poor solubility and the polydisperse nature of the material.

Conclusion

A series of macrocycles consisting of diacetylene interlinked *meta*-benzene corner units was synthesized and fully characterized. The number and the relative position of perfluorinated corner units were varied systematically to investigate the strength of intermolecular interactions arising from benzene/tetrafluorobenzene quadrupole interactions. In particular, concentration dependent ^{1}H-NMR experiments and vapour pressure osmometry investigations provided insight into the aggregation behaviour of these SPMs in $CHCl_3$. While no aggregation tendency was observed for the unfluorinated SPM **1**, already a single fluorinated corner unit in SPM **2** resulted in the formation of larger aggregates. Interestingly, the formation of aggregates beyond dimers have

only been observed for this SPM **2** comprising a single fluorinated corner subunit while for all the other SPMs **3–6** comprising several fluorinated corner units, all concentration dependent investigations pointed towards dimerization as the major aggregation process. Thermodynamic data of the aggregation processes of these SPMs were obtained by studying their assembly behaviour at various temperatures. According to these results, the aggregation of these SPMs **2–6** comprising fluorinated corner units is enthalpically driven. The largest enthalpic contribution together with the largest entropic loss was observed for SPM **3** having two fluorinated corner units facing each other. Furthermore, by heating a concentrated solution of SPM **3** in toluene to 50 °C a precipitation of rod-like crystallites with a hexagonal section was observed. Investigation of these crystallites by SEM displayed electron beam induced healing features which have – to the best of our knowledge – not been reported so far for organic materials. Further analysis of the crystallite forming material pointed at covalently interlinked macrocycles, probably arising from temperature induced oligomerization in the supramolecular stack.

Currently, we are investigating potential applications of these crystallites displaying promising conducting properties in the SEM experiment.

Experimental

General

All reagents were obtained from Aldrich or ABCR and were used without further purification. Solvents were distilled and – if mentioned – dried by standard methods.[90] Unless otherwise stated, the reactions were performed under a N_2 atmosphere. Compounds **9**, **11**, **12**, **18**, **19** and **20** were prepared according to already reported procedures.[19] Thin layer chromatography (TLC) was carried out on Merck silica gel 60 F254 plates and Merck silica gel 60 (0.040–0.063 mm) was used for column chromatography (CC). Preparative size exclusion chromatography was performed with Bio-Beads® S-X Beads from *BIO RAD* and distilled toluene as eluent. ^{1}H-NMR and ^{13}C-NMR spectra were recorded on a Bruker Ultra Shield 300 MHz and 500 MHz NMR spectrometer, the *J* values are given in Hz. MALDI-TOF MS spectra were recorded on a PerSeptive Biosystems Voyager-DE PRO time-of-flight mass spectrometer. EI-MS were recorded on a Finnigan MAT 95Q mass spectrometer. Elemental analyses (EA) were recorded using a ThermoQuest FlashEA 1112 N/Protein Analyzer. Vapour pressure osmometry experiments were performed with a KNAUER vapour pressure osmometer K-7000. A LEO 1530 scanning electron microscope was used for scanning electron microscopy (SEM) investigations. Furthermore, a 10 kV acceleration voltage and a 100 pA beam current were used to record the sample. The secondary electrons were detected with an in-lens detector while the sample surface was scanned for crystallites.

1,3-Bis(bromoethynyl)benzene 8. 1,3-Diethynylbenzene (**7**) (1.50 g, 11.9 mmol), *N*-bromosuccinimide (6.00 g, 33.7 mmol) and silver nitrate (354 mg, 2.09 mmol) were dissolved in acetone (90 mL). The reaction mixture was stirred for 2 hours at room temperature, then adsorbed on silica gel and purified by CC to yield **8** (2.60 g, 77%). ^{1}H-NMR (300 MHz, $CDCl_3$) δ 7.26 (t, 1H, ArH), 7.42 (m, 2H, ArH), 7.53 (s, 1H, ArH). ^{13}C-NMR (75 MHz, $CDCl_3$) δ 51.01, 78.99, 122.98, 128.38, 132.02, 135.24. *m/z* (EI) 283.8 [M^+]. EA calc. for $C_{10}H_4Br_2$ (283.95): C 42.30, H 1.42. Found: C 42.42; H 1.49%.

1,3-Bis(bromoethynyl)-5-hexylbenzene 10. 1,3-Diethynyl-5-hexylbenzene (**9**) (700 mg, 3.33 mmol), *N*-bromosuccinimide (1.20 g, 6.75 mmol) and silver nitrate (100 mg, 0.589 mmol) were dissolved in acetone (30 mL). The reaction mixture was stirred for 2 hours at room temperature, then adsorbed on silica gel and purified by CC to yield **10** (1.11 g, 91%). ^{1}H-NMR (300 MHz, $CDCl_3$) δ 0.89 (t, 3H, $^3J_{HH}$ = 6.6 Hz, CH_3), 1.29 (br, 6H), 1.57 (m, 2H), 2.54 (t, 2H, $^3J_{HH}$ = 7.65 Hz, -CH_2Ar), 7.24 (br, 2H, ArH), 7.34 (t, *J* = 1.35 Hz, 1H, $^3J_{HH}$ = 1.35 Hz, ArH). ^{13}C-NMR (75 MHz, $CDCl_3$) δ 14.07, 22.54, 28.78, 30.96, 31.61, 35.33, 50.28, 79.25, 122.75, 132.27, 132.59, 143.36. EA calc. for $C_{16}H_{16}Br_2$ (368.11): C 52.21, H 4.38. Found: C 52.55; H 4.17%.

1,3-Bis((3-hexyl-5-((triisopropylsilyl)ethynyl)phenyl)buta-1,3-diynyl)benzene 13. In degassed diisopropylethylamine (4 mL), **8** (1.42 g, 5.00 mmol), $Pd_2(dba)_3{\cdot}CHCl_3$ (80.0 mg, 0.0770 mmol) and CuI (50.0 mg, 0.260 mmol) were added. Subsequently, to this mixture a solution of **11** (4.00 g, 11.0 mmol) in dry and degassed toluene (30 mL) was added dropwise in 2 hours at room temperature. After stirring for another 2 hours, the solvent was removed. The residue was purified by CC (silica gel, hexane) to give the desired product **13** (2.82 g, 66%) as a yellow solid. ^{1}H-NMR (300 MHz, $CDCl_3$) δ 0.92 (t, 6H, $^3J_{HH}$ = 6.3 Hz, CH_3), 1.15 (s, 42H), 1.35 (br, 12H), 1.65 (q, 4H), 2.58 (t, 4H, $^3J_{HH}$ = 7.8 Hz, $ArCH_2$), 7.30 (br, 5H, ArH), 7.48 (br, 3H, ArH), 7.52 (m, 1H, ArH), 7.67 (t, 1H, $^3J_{HH}$ = 1.35, ArH). ^{13}C-NMR (75 MHz, $CDCl_3$) δ 11.45, 13.98, 18.68, 22.55, 28.88, 30.99, 31.65, 35.48, 73.90, 74.93, 80.34, 81.70, 91.48, 106.22, 121.77, 122.62, 124.06, 128.69, 132.27, 132.93, 133.00, 133.46, 136.17, 143.51. *m/z* (MALDI-TOF) 854.45 [M^+]. EA calc. for $C_{60}H_{78}Si_2$ (855.43): C 84.24, H 9.19. Found: C 84.22, H, 9.38%.

1,3-Bis((3-ethynyl-5-hexylphenyl)buta-1,3-diynyl)benzene 14. TBAF (765 mg, 2.93 mmol) in THF (15 mL) was added dropwise, over a period of 30 minutes, to a stirred solution of **13** (1.00 g, 1.17 mmol) in wet (containing 1% of water) THF (150 mL). After stirring for 4 hours at room temperature the solvent was removed and the residue was chromatographed (silica gel, hexane) to give the desired product **14** (0.52 g, 81%) as colourless oil. ^{1}H-NMR (300 MHz, $CDCl_3$) δ 0.89 (t, 6H, $^3J_{HH}$ = 6.75 Hz, CH_3), 1.33 (br, 12H), 1.61 (br, 4H), 2.56 (t, 4H, $^3J_{HH}$ = 7.65 Hz, $ArCH_2$), 7.34 (br, 5H, ArH), 7.50 (br, 4H, ArH), 7.68 (t, 1H, $^3J_{HH}$ = 1.5 Hz, ArH). ^{13}C-NMR (75 MHz, $CDCl_3$) δ 14.04, 22.53, 28.80, 30.91, 31.60, 35.33, 73.92, 74,76, 77.72, 80.28, 81.30, 82.65, 121.68, 122.28, 122.42, 128.63, 132.76, 132.99, 133.04, 133.24, 136.06, 143.48. EI: *m/z* 542.2 [M^+]. EA calc. for $C_{42}H_{38}$ (542.75): C 92.94, H 7.06. Found: C 92.88, H 7.12%.

1,3-Bis((3-(bromoethynyl)-5-hexylphenyl)buta-1,3-diynyl)benzene 15. **14** (3.13 g, 50.0 mmol), *N*-bromosuccinimide (19.6 g, 110 mmol) and silver nitrate (1.64 g, 9.66 mmol) were dissolved in acetone (80 mL). The reaction mixture was stirred for 2 hours at room temperature, then adsorbed on silica gel and purified by CC to yield in the desired product **15** (3.29 g, 94%). ^{1}H-NMR (300 MHz, $CDCl_3$) δ 0.92 (t, 6H, $^3J_{HH}$ = 6.3 Hz, -CH_3), 1.33 (br, 12H), 1.60 (m, 4H), 2.56 (t, 4H, $^3J_{HH}$ = 7.7 Hz, -CH_2Ar),

7.28 (m, 2H, ArH), 7.33 (m, 2H, ArH), 7.36 (m, 1H, ArH), 7.43 (m, 2H, ArH), 7.52 (m, 2H, ArH), 7.67 (m, 1H, ArH). ^{13}C-NMR (75 MHz, $CDCl_3$) δ 14.06, 22.54, 28.80, 30.90, 31.61, 35.33, 50.63, 73.97, 74.76, 79.14, 80.31, 81.24, 121.71, 122.27, 122.96, 128.62, 132.67, 133.91, 132.99, 133.05, 136.06, 143.51. *m/z* (MALDI-TOF) 698.10 [M$^+$]. EA calc. for $C_{42}H_{36}Br_2$ (700.54): C 72.01, H 5.18. Found: C 71.54, H 5.60%.

(5,5′-(5-Hexyl-1,3-phenylene)bis(buta-1,3-diyne-4,1-diyl)bis(3-hexyl-5,1-phenylene))bis(ethyne-2,1-diyl)bis(triisopropylsilane) 16. **10** (200 mg, 0.540 mmol), $Pd_2(dba)_3{\cdot}CHCl_3$ (80.0 mg, 0.0770 mmol) and CuI (50.0 mg, 0.260 mmol) was suspended in dry and degassed diisopropylethylamine (4 mL). Subsequently, a solution of **11** (400 mg, 1.100 mmol) in toluene (30 mL) was dropped to the reaction mixture over a period of 2 hours. The reaction mixture was stirred for another 2 hours at room temperature, the solvent was removed and the crude purified by CC (silica gel, hexane) to yield the desired product **16** (120 mg, 24%). ^{1}H-NMR (300 MHz, $CDCl_3$) δ 0.91 (t, 9H, $^3J_{HH} = 6.45$ Hz, -CH_3), 1.15 (s, 42H), 1.32 (m, 18H), 1.62 (m, 6H), 2.60 (t, 6H, $^3J_{HH} =$ 7.65 Hz, -CH_2Ar), 7.33 (br, 6H, ArH), 7.50 (br, 3H, ArH). ^{13}C-NMR (75 MHz, $CDCl_3$) δ 11.25, 14.09, 18.65, 22.57, 28.79, 28.88, 30.93, 31.08, 31.63, 31.64, 35.37, 35.43, 73.84, 74.28, 80.60, 81.29, 91.20, 106.00, 121.60, 122.09, 123.81, 132.24, 132.85, 133.24, 133.39, 143.40, 143.66. *m/z* (MALDI-TOF) 1875.04 [2M$^+$]. EA calc. for $C_{66}H_{90}Si_2$ (939.59): C 84.37, H 9.65. Found: C 83.62, H 9.91%.

5,5′-(5-Hexyl-1,3-phenylene)bis(buta-1,3-diyne-4,1-diyl)bis(1-ethynyl-3-hexylbenzene) 17. TBAF (379 mg, 1.45 mmol) in THF (10 mL) was added dropwise, over a period of 30 minutes, to a stirred solution of **16** (550 mg, 0.580 mmol) in THF (40 mL). After stirring for 4 hours at room temperature the solvent was removed and the residue was chromatographed (silica gel, hexane) to give the desired product **17** (0.35 g, 96%) as a colourless oil. ^{1}H-NMR (300 MHz, $CDCl_3$) δ 0.89 (t, 9H, $^3J_{HH} = 6.3$ Hz, CH_3), 1.30 (br, 18H), 1.60 (m, 6H), 2.56 (t, 6H, $^3J_{HH} = 7.8$ Hz, CH_2Ar), 3.08 (s, 2H), 7.32 (m, 6H, ArH), 7.48 (m, 3H, ArH). ^{13}C-NMR (75 MHz, $CDCl_3$) δ 14.06, 22.54, 28.80, 30.90, 30.95, 31.61, 35.36, 74.00, 74.26, 77.68, 80.70, 81.06, 82.67, 121.78, 122.05, 122.42, 132.80, 133.02, 133.26, 133.50, 143.51, 143.67. *m/z* (MALDI-TOF) 626.21 [M$^+$]. EA calc. for $C_{48}H_{50}$ (626.91): C 91.96, H 8.04. Found: C 91.25, H 8.15%.

Shape-persistent macrocycle (SPM) 1. To a suspension of $Cu(OAc)_2{\cdot}H_2O$ (150 mg, 0.753 mmol) in pyridine (300 mL) and benzene (200 mL) a solution of **14** (100 mg, 0.180 mmol) in benzene (100 mL) was added dropwise, at room temperature, over a period of 24 hours. After addition, the reaction mixture was stirred for an additional two days at room temperature. The reaction mixture was concentrated and filtered and evaporated to dryness. The crude was purified by size exclusion chromatography (SEC) to yield the desired SPM **1** (25 mg, 25%) as a brown solid. ^{1}H-NMR (300 MHz, $CDCl_3$) δ 0.91 (t, 12H, $^3J_{HH} = 6.6$ Hz, CH_3), 1.25 (br, 24H), 1.56 (m, 8H), 2.57 (t, 8H, $^3J_{HH} = 7.65$ Hz, $ArCH_2$), 7.32 (br, 10H, ArH), 7.50 (m, 8H, ArH), 7.74 (m, 2H, ArH). ^{13}C-NMR (75 MHz, $CDCl_3$) δ 14.11, 22.58, 28.81, 30.97, 31.65, 35.43, 74.18, 74.28, 74.75, 80.43, 80.83, 81.05, 121.90, 122.00, 122.40, 128.74, 132.70, 132.80, 132.83, 134.30, 136.95, 143.72. *m/z* (MALDI-TOF) 1079.94 [M$^+$]. EA calc for $C_{84}H_{72}$ (1081.47): C 93.29, H 6.71. Found: C 92.67, H 6.68%.

SPM 2. To a degassed solution of diisopropylethylamine (5 mL), dry toluene (450 mL), $Pd_2(dba)_3{\cdot}CHCl_3$ (40.0 mg, 0.0390 mmol) and CuI (20.0 mg, 0.100 mmol) a solution of **15** (158 mg, 0.120 mmol) and **19** (139 mg, 0.120 mmol) in dry toluene (40 mL) was added dropwise over a period of 10 hours under a nitrogen atmosphere. The reaction mixture was stirred for 4 days at room temperature, the solvent was removed, and the residue was dissolved in toluene (15 mL), filtered and purified by SEC (toluene) to give the desired SPM **2** (10.4 mg, 9%) as a brown solid. ^{1}H-NMR (300 MHz, $CDCl_3$) δ 0.90 (t, 12H, $^3J_{HH} = 6.45$ Hz, CH_3), 1.31 (br, 24H), 1.58 (br, 8H), 2.59 (t, 8H, $^3J_{HH} = 7.65$ Hz, CH_2Ar), 7.31 (br, 5H, ArH), 7.33 (s, 4H, ArH), 7.46 (br, 2H, ArH), 7.56 (br, 2H, ArH), 7.58 (s, 2H, ArH), 7.72 (br, 1H, ArH). ^{13}C-NMR (75 MHz, $CDCl_3$) δ 14.02, 22.52, 28.87, 30.86, 31.61, 35.39, 65.41, 73.46, 74.25, 74.31, 74.54, 74.79, 80.43, 80.59, 80.93, 81.05, 83.85, 84.75, 121.35, 122.11, 122.35, 122.44, 122.52, 128.61, 132.59, 132.84, 132.92, 133.26, 133.38, 134.38, 134.46, 136.88, 143.69, 143.84. ^{19}F-NMR (376 MHz, $CDCl_3$) δ −105.38, −124.85, −162.15. *m/z* (MALDI-TOF) 1152.53 [M$^+$]. EA calc. for $C_{84}H_{68}F_4$ (1152.53): C 87.47, H 5.95. Found: C 85.33, H 6.34%.

SPM 3. To a solution of $Pd(PPh_3)_2Cl_2$ (300 mg, 0.430 mmol), CuI (400 mg, 2.10 mmol) and dry silica gel in diisopropylethylamine (15 mL) and dry THF (1200 mL), a solution of **19** (200 mg, 0.320 mmol) in dry THF (100 mL) was added dropwise over a period of 10 hours. The reaction mixture was stirred for 4 days under dry air at room temperature. The solvent was removed, and the residue was dissolved in toluene (15 mL), filtered over 1 cm silica gel and purified by SEC to yield the desired SPM **3** (40 mg, 20%) as a yellow solid. ^{1}H-NMR (300 MHz, $CDCl_3$) δ 0.92 (t, 12H, $^3J_{HH} = 6.3$ Hz, CH_3), 1.33 (br, 24H), 1.65 (m, 8H), 2.57 (t, 8H, $^3J_{HH} = 7.5$ Hz, CH_2Ar), 7.29 (s, 8H), 7.54 (s, 4H). ^{13}C-NMR (125 MHz, d_8-toluene, 50 °C) δ 14.1, 22.8, 29.2, 31.0, 32.0, 35.5, 66.1, 74.3, 75.5, 81.4, 84.5, 85.5 (m), 100.0 (m), 121.9, 122.8, 132.9, 133.4, 134.9, 137.3 (*J* 255), 143.9, 152.5 (*J* 255), 161.0 (*J* 255). ^{19}F-NMR (376 MHz, $CDCl_3$) δ −106.2, −125.7, −162.6. *m/z* (EI) 1224.5 [M$^+$]. EA calc. for $C_{84}H_{64}F_8$ (1224.4): C 82.33, H 5.27. Found: C 81.97, H 5.24%.

6,6′-(5,5′-(Perfluoro-1,3-phenylene)bis(buta-1,3-diyne-4,1-diyl)-bis(3-hexyl-5,1-phenylene))bis(buta-1,3-diyne-4,1-diyl)bis(2-(bromo-ethynyl)-1,3,4,5-tetrafluorobenzene) 20. **12** (2.00 g, 5.60 mmol), $Pd_2(dba)_3{\cdot}CHCl_3$ (120 mg, 0.110 mmol) and CuI (50.0 mg, 0.260 mmol) were dissolved in dry and degassed diisopropylethylamine (4 mL). Subsequently, to the reaction mixture a solution of **17** (450 mg, 0.720 mmol) in dry toluene (30 mL) was added dropwise over a period of 2 hours at room temperature. The reaction mixture was stirred for another 2 hours, the solvent was removed and the residue was purified by CC (silica gel, hexane) to yield the desired product **20** (380 mg, 46%) as a yellow solid.: ^{1}H-NMR (300 MHz, $CDCl_3$) δ 0.90 (m, 9H), 1.32 (br, 18H), 1.61 (m, 6H), 2.58 (t, 6H, $^3J_{HH} = 7.65$ Hz, CH_2Ar), 7.33 (s, 2H, ArH), 7.35 (s, 4H, ArH), 7.46 (m, 1H, ArH), 7.48 (m, 2H, ArH). ^{13}C-NMR (75 MHz, $CDCl_3$) δ 14.05, 22.57, 28.84, 30.89, 31.64, 35.36, 62.75 (q), 64.80 (t), 65.43 (t), 73.32 (d), 74.18, 74.45, 80.58, 80.95, 83.74, 84.45 (q), 99.60 (m), 121.19, 121.97, 122.18, 133.28, 133.30, 133.51, 133.60, 133.84, 137.25

(*J* 254), 143.72, 143.85, 152.35 (*J* 262.5), 160.0 (*J* 255.0). ^{19}F-NMR (376 MHz, $CDCl_3$) δ −106.9 (d), −125.3 (m), −162.4 (m). EA calc. for $C_{68}H_{48}Br_2F_8$ (1176.90): C 69.40, H 4.11. Found: C 69.24, H 4.45%.

SPM 4. To a solution of $Pd_2(dba)_3{\cdot}CHCl_3$ (40.0 mg, 0.0390 mmol) and CuI (20.0 mg, 0.100 mmol) in diisopropylethylamine (5 mL) and dry toluene (450 mL), a solution of **9** (140 mg, 0.120 mmol) and **20** (25.0 mg, 0.120 mmol) in dry toluene (40 mL) was added dropwise over a period of 10 hours under a nitrogen atmosphere. After 4 days the reaction mixture was evaporated, the crude was dissolved in toluene (15 mL), filtered and purified by SEC (toluene) to give the desired SPM **4** (13 mg, 9%) as a brown solid. ^{1}H-NMR (300 MHz, $CDCl_3$) δ 0.94 (m, 12H), 1.34 (br, 24H), 1.53 (br, 8H), 2.34 (m, 8H), 6.71 (br, 2H), 6.92 (s, 2H), 6.94 (br, 2H), 7.13 (br, 2H), 7.19 (m, 2H), 7.36 (br, 2H). ^{13}C-NMR (125 MHz, $CDCl_3$) δ 14.12, 22.70, 28.72, 31.03, 31.73, 35.55, 65.33, 65.59, 73.54 (d), 73.93, 74.68, 80.4, 80.62, 83.41, 83.64, 84.76, 85.20, 99.02 (m), 99.86 (m), 121.26, 121.49, 121.97, 122.26, 131.09, 131.40, 131.76, 132.61, 133.15, 134.10, 135.11, 135.87, 136.44 (*J* 277), 143.20, 143.40, 143.61, 151.05 (*J* 262), 152.06 (*J* 259), 161.32 (*J* 263). ^{19}F-NMR (376 MHz, $CDCl_3$) δ −103.83 (s), −104.93 (s), −124.69 (m), −162.44 (d). *m/z* (MALDI-TOF) 1223.57 $[M - H]^+$, 2451.47 $[2M + 2H]^+$. EA calc. for $C_{84}H_{64}F_8$ (1224.4): C 82.33, H 5.27. Found: C 82.07, H 5.44%.

SPM 6. To a solution of $Pd_2(dba)_3{\cdot}CHCl_3$ (50.0 mg, 0.0480 mmol) and CuI (20.0 mg, 0.100 mmol) in diisopropylethylamine (5 mL) and dry toluene (850 mL), a solution of **19** (76.6 mg, 0.125 mmol) and **21** (145 mg, 0.125 mmol) in dry toluene (40 mL) was added dropwise over a period of 10 hours under a nitrogen atmosphere. After 4 days the reaction mixture was evaporated, the crude was dissolved in toluene (15 mL), filtered and purified by SEC (toluene) to give the desired SPM **6** (12 mg, 6%) as a brown solid. ^{1}H-NMR (300 MHz, $CDCl_3$) δ 0.94 (t, 12H, $^3J_{HH}$ = 6.6 Hz, CH_3), 1.35 (br, 24H), 1.59 (m, 8H), 2.53 (t, 8H, $^3J_{HH}$ = 7.5 Hz, CH_2Ar), 7.13 (s, 8H, ArH), 7.63 (s, 4H, ArH). ^{13}C-NMR (125 MHz, $CDCl_3$) δ 13.91, 22.47, 28.75, 30.68, 31.56, 35.32, 65.70 (d), 73.84 (d), 83.71 (d), 84.90 (d), 99.73 (m), 121.53, 132.19, 136.23, 137.04 (*J* 325.0), 144.04, 152.11 (*J* 237.5), 161.26 (*J* 276.5). ^{19}F-NMR (376 MHz, $CDCl_3$) δ −105.18 (d), −124.36 (t), −161.38 (d). *m/z* (MALDI-TOF) 1617.87 $[M + H]^+$. EA calc. for $C_{104}H_{64}F_{16}$ (1617.6): C 77.22, H 3.99. Found: C 77.54, H 3.86%.

Sample preparation for SEM

A dispersion of the precipitate obtained by heating SPM **3** in toluene was prepared by mixing a few micrograms of the precipitate in 1 mL isopropanol under mild sonication for 1 min. 10 µL of the dispersion were spin-cast at 5000 rpm for 90 s onto a native silicon substrate. The sample was subsequently investigated by SEM.

Acknowledgements

The authors acknowledge the support with a post doctoral position for L. S. by the Center for Functional Nanostructures (CFN) of the Deutsche Forschungsgemeinschaft (DFG) within project C3. M. M. and M. M. acknowledge support from the Swiss National Science Foundation (SNSF) and the Innovation Promotion Agency (CTI). The authors thank Prof. Thomas Ward for proof reading of the manuscript.

References

1 C. Grave and A. D. Schluter, *Eur. J. Org. Chem.*, 2002, 3075–3098.
2 D. Zhao and J. S. Moore, *Chem. Commun.*, 2003, 807–818.
3 Y. Yamaguchi and Z.-i. Yoshida, *Chem. Eur. J.*, 2003, **9**, 5430–5440.
4 S. Hoeger, *Chem. Eur. J.*, 2004, **10**, 1320–1329.
5 W. Zhang and J. S. Moore, *Angew. Chem., Int. Ed.*, 2006, **45**, 4416–4439.
6 M. J. MacLachlan, *Pure Appl. Chem.*, 2006, **78**, 873–888.
7 Z.-T. Li, J.-L. Hou, C. Li and H.-P. Yi, *Chem. Asian J.*, 2006, **1**, 766–778.
8 M. Fischer, G. Lieser, A. Rapp, I. Schnell, W. Mamdouh, S. De Feyter, F. C. De Schryver and S. Hoeger, *J. Am. Chem. Soc.*, 2004, **126**, 214–222.
9 M. Venturi, V. Balzani, F. Marchioni, D. M. Opris, P. Franke and A. D. Schluter, *Macrocyclic Chemistry*, ed. K. Gloe, Springer, Netherlands, 2005, pp. 219–234.
10 M. Venturi, F. Marchioni, B. F. Ribera, V. Balzani, D. M. Opris and A. D. Schluter, *ChemPhysChem*, 2006, **7**, 229–239.
11 M. Fischer and S. Hoeger, *Eur. J. Org. Chem.*, 2003, 441–446.
12 M. Fischer and S. Hoeger, *Tetrahedron*, 2003, **59**, 9441–9446.
13 U. Lehmann and A. D. Schluter, *Eur. J. Org. Chem.*, 2000, 3483–3487.
14 Y. Tobe, N. Utsumi, A. Nagano and K. Naemura, *Angew. Chem., Int. Ed.*, 1998, **37**, 1285–1287.
15 P. N. W. Baxter, *Chem. Eur. J.*, 2003, **9**, 5011–5022.
16 L. He, Y. An, L. Yuan, W. Feng, M. Li, D. Zhang, K. Yamato, C. Zheng, X. C. Zeng and B. Gong, *Proc. Natl. Acad. Sci. U. S. A.*, 2006, **103**, 10850–10855.
17 S. Klyatskaya, N. Dingenouts, C. Rosenauer, B. Mueller and S. Hoeger, *J. Am. Chem. Soc.*, 2006, **128**, 3150–3151.
18 S. H. Seo, T. V. Jones, H. Seyler, J. O. Peters, T. H. Kim, J. Y. Chang and G. N. Tew, *J. Am. Chem. Soc.*, 2006, **128**, 9264–9265.
19 L. Shu and M. Mayor, *Chem. Commun.*, 2006, 4134–4136.
20 D. Borissov, A. Ziegler, S. Hoeger and W. Freyland, *Langmuir*, 2004, **20**, 2781–2784.
21 G.-B. Pan, X.-H. Cheng, S. Hoeger and W. Freyland, *J. Am. Chem. Soc.*, 2006, **128**, 4218–4219.
22 J. S. Moore, *Acc. Chem. Res.*, 1997, **30**, 402–413.
23 K. Nakao, M. Nishimura, T. Tamachi, Y. Kuwatani, H. Miyasaka, T. Nishinaga and M. Iyoda, *J. Am. Chem. Soc.*, 2006, **128**, 16740–16747.
24 S. Hoeger, X. H. Cheng, A.-D. Ramminger, V. Enkelmann, A. Rapp, M. Mondeshki and I. Schnell, *Angew. Chem., Int. Ed.*, 2005, **44**, 2801–2805.
25 T. Zhao, Z. Liu, Y. Song, W. Xu, D. Zhang and D. Zhu, *J. Org. Chem.*, 2006, **71**, 7422–7432.
26 A. S. Shetty, J. Zhang and J. S. Moore, *J. Am. Chem. Soc.*, 1996, **118**, 1019–1027.
27 J. Zhang and J. S. Moore, *J. Am. Chem. Soc.*, 1992, **114**, 9701–9702.
28 S. Hoeger, K. Bonrad, A. Mourran, U. Beginn and M. Moeller, *J. Am. Chem. Soc.*, 2001, **123**, 5651–5659.
29 Y. Tobe, N. Utsumi, K. Kawabata, A. Nagano, K. Adachi, S. Araki, M. Sonoda, K. Hirose and K. Naemura, *J. Am. Chem. Soc.*, 2002, **124**, 5350–5364.
30 C.-H. Lin and J. Tour, *J. Org. Chem.*, 2002, **67**, 7761–7768.
31 H. Sugiura, Y. Takahira and M. Yamaguchi, *J. Org. Chem.*, 2005, **70**, 5698–5708.
32 K. Nakamura, H. Okubo and M. Yamaguchi, *Org. Lett.*, 2001, **3**, 1097–1099.
33 M.-F. Ng and S.-W. Yang, *J. Phys. Chem. B*, 2007, **111**, 13886–13893.
34 C. R. Patrick and G. S. Prosser, *Nature*, 1960, **187**, 1021.
35 W. Vanspeybrouck, W. A. Herrebout, B. J. Van Der Veken, J. Lundell and R. N. Perutz, *J. Phys. Chem. B*, 2003, **107**, 13855–13861.
36 F. Cozzi, F. Ponzini, R. Annunziata, M. Cinquini and J. S. Siegel, *Angew. Chem., Int. Ed.*, 1995, **34**, 1019–1020.
37 F. Cozzi and J. S. Siegel, *Pure Appl. Chem.*, 1995, **67**, 683–689.
38 H. Adams, C. A. Hunter, K. R. Lawson, J. Perkins, S. E. Spey, C. J. Urch and J. M. Sanderson, *Chem. Eur. J.*, 2001, **7**, 4863–4877.
39 S. L. Cockroft, C. A. Hunter, K. R. Lawson, J. Perkins and C. J. Urch, *J. Am. Chem. Soc.*, 2005, **127**, 8594–8595.
40 S. L. Cockroft, J. Perkins, C. Zonta, H. Adams, S. E. Spey, C. M. R. Low, J. G. Vinter, K. R. Lawson, C. J. Urch and C. A. Hunter, *Org. Biomol. Chem.*, 2007, **5**, 1062–1080.

41 S. Bacchi, M. Benaglia, F. Cozzi, F. Demartin, G. Filippini and A. Gavezzotti, *Chem. Eur. J.*, 2006, **12**, 3538–3546.
42 C. A. Hunter, K. R. Lawson, J. Perkins and C. J. Urch, *J. Chem. Soc., Perkin Trans. 2*, 2001, 651–669.
43 E. A. Meyer, R. K. Castellano and F. Diederich, *Angew. Chem., Int. Ed.*, 2003, **42**, 1210–1250.
44 S. Tsuzuki, T. Uchimaru and M. Mikami, *J. Phys. Chem. A*, 2006, **110**, 2027–2033.
45 J. Kendall, R. McDonald, M. J. Ferguson and R. R. Tykwinski, *Org. Lett.*, 2008, **10**, 2163–2166.
46 W. J. Feast, P. W. Lovenich, H. Puschmann and C. Taliani, *Chem. Commun.*, 2001, 505–506.
47 J. C. Collings, A. S. Batsanov, J. A. K. Howard, D. A. Dickie, J. A. C. Clyburne, H. A. Jenkins and T. B. Marder, *J. Fluorine Chem.*, 2005, **126**, 515–519.
48 C. E. Smith, P. S. Smith, R. L. Thomas, E. G. Robins, J. C. Collings, C. Dai, A. J. Scott, S. Borwick, A. S. Batsanov, S. W. Watt, S. J. Clark, C. Viney, J. A. K. Howard, W. Clegg and T. B. Marder, *J. Mater. Chem.*, 2004, **14**, 413–420.
49 S. Meejoo, B. M. Kariuki and K. D. M. Harris, *ChemPhysChem*, 2003, **4**, 766–769.
50 J. C. Collings, K. P. Roscoe, E. G. Robins, A. S. Batsanov, L. M. Stimson, J. A. K. Howard, S. J. Clark and T. B. Marder, *New J. Chem.*, 2002, **26**, 1740–1746.
51 W. Jankowski, M. Gdaniec and T. Polonski, *Acta Crystallogr., Sect. C: Cryst. Struct. Commun.*, 2006, **C62**, o492-o494.
52 F. Ponzini, R. Zagha, K. Hardcastle and J. S. Siegel, *Angew. Chem., Int. Ed.*, 2000, **39**, 2323–2325.
53 S. Zhu, S. Zhu, G. Jin and Z. Li, *Tetrahedron Lett.*, 2005, **46**, 2713–2716.
54 D. M. Cho, S. R. Parkin and M. D. Watson, *Org. Lett.*, 2005, **7**, 1067–1068.
55 L. S. Reddy, A. Nangia and V. M. Lynch, *Cryst. Growth Des.*, 2004, **4**, 89–94.
56 M. Gdaniec, W. Jankowski, M. J. Milewska and T. Polonski, *Angew. Chem., Int. Ed.*, 2003, **42**, 3903–3906.
57 J. Liu, E. M. Murray and V. G. Young, Jr., *Chem. Commun.*, 2003, 1904–1905.
58 V. R. Vangala, A. Nangia and V. M. Lynch, *Chem. Commun.*, 2002, 1304–1305.
59 L. Shu, Z. Mu, H. Fuchs, L. Chi and M. Mayor, *Chem. Commun.*, 2006, 1862–1863.
60 G. W. Coates, A. R. Dunn, L. M. Henling, J. W. Ziller, E. B. Lobkovsky and R. H. Grubbs, *J. Am. Chem. Soc.*, 1998, **120**, 3641–3649.
61 G. W. Coates, A. R. Dunn, L. M. Henling, D. A. Dougherty and R. H. Grubbs, *Angew. Chem., Int. Ed.*, 1997, **36**, 248–251.
62 R. Xu, V. Gramlich and H. Frauenrath, *J. Am. Chem. Soc.*, 2006, **128**, 5541–5547.
63 Y. El-azizi, A. Schmitzer and S. K. Collins, *Angew. Chem., Int. Ed.*, 2006, **45**, 968–973.
64 M. J. Marsella, Z.-Q. Wang, R. J. Reid and K. Yoon, *Org. Lett.*, 2001, **3**, 885–887.
65 S. W. Watt, C. Dai, A. J. Scott, J. M. Burke, R. L. Thomas, J. C. Collings, C. Viney, W. Clegg and T. B. Marder, *Angew. Chem., Int. Ed.*, 2004, **43**, 3061–3063.
66 K. Kishikawa, K. Oda, S. Aikyo and S. Kohmoto, *Angew. Chem., Int. Ed.*, 2007, **46**, 764–768.
67 M. Weck, A. R. Dunn, K. Matsumoto, G. W. Coates, E. B. Lobkovsky and R. H. Grubbs, *Angew. Chem., Int. Ed.*, 1999, **38**, 2741–2745.
68 K. B. Woody, J. E. Bullock, S. R. Parkin and M. D. Watson, *Macromolecules*, 2007, **40**, 4470–4473.
69 A. F. M. Kilbinger and R. H. Grubbs, *Polym. Mater. Sci. Eng.*, 2001, **85**, 350–351.
70 A. F. M. Kilbinger and R. H. Grubbs, *Angew. Chem., Int. Ed.*, 2002, **41**, 1563–1566.
71 K. Kasai and M. Fujita, *Chem. Eur. J.*, 2007, **13**, 3089–3105.
72 Y. Sonoda, M. Goto, S. Tsuzuki and N. Tamaoki, *J. Phys. Chem. A*, 2007, **111**, 13441–13451.
73 M. Morimoto, S. Kobatake and M. Irie, *Cryst. Growth Des.*, 2003, **3**, 847–854.
74 T. Gray, T.-D. Kim, D. B. Knorr, Jr., J. Luo, A. K. Y. Jen and R. M. Overney, *Nano Lett.*, 2008, **8**, 754–759.
75 E. A. Meyer, R. K. Castellano and F. Diederich, *Angew. Chem., Int. Ed.*, 2003, **42**, 1210–1250.
76 A. Zahn, C. Brotschi and C. J. Leumann, *Chem. Eur. J.*, 2005, **11**, 2125–2129.
77 G. Mathis and J. Hunziker, *Angew. Chem., Int. Ed.*, 2002, **41**, 3203–3205.
78 B. C. Gorske and H. E. Blackwell, *J. Am. Chem. Soc.*, 2006, **128**, 14378–14387.
79 S. Lahiri, J. L. Thompson and J. S. Moore, *J. Am. Chem. Soc.*, 2000, **122**, 11315–11319.
80 C. Glaser, *Ber. Dtsch. Chem. Ges.*, 1869, **2**, 422–424.
81 P. Siemsen, R. C. Livingston and F. Diederich, *Angew. Chem., Int. Ed.*, 2000, **39**, 2632–2657.
82 P. Cadiot and W. Chodkiewicz, *Chem. Acetylenes*, 1969, 597–647.
83 K. Sonogashira, Y. Tohda and N. Hagihara, *Tetrahedron Lett.*, 1975, 4467–4470.
84 K. Sonogashira, in *Metal-Catalyzed Cross-Coupling Reactions*, ed. F. Diederich and P. J. Stang, Wiley-VCH, Weinheim, 1998, pp. 203–229.
85 E. J. Corey and P. L. Fuchs, *Tetrahedron Lett.*, 1972, 3769–3772.
86 J. Wityak and J. B. Chan, *Synth. Commun.*, 1991, **21**, 977–979.
87 R. Rossi, A. Carpita and C. Bigelli, *Tetrahedron Lett.*, 1985, **26**, 523–526.
88 I. Horman and B. Dreux, *Helvetica Chimica Acta*, 1984, **67**, 754–764.
89 R. Xu, W. B. Schweizer and H. Frauenrath, *J. Am. Chem. Soc.*, 2008, **130**, 11437–11445.
90 W. L. F. Armarego and C. L. L. Chai, *Purification of Laboratory Chemicals*, Butterworth Heinemann, Amsterdam, Boston, London, New York, Oxford, Paris, San Diego, San Francisco, Singapore, Sydney, Tokyo, 5th edn, 2003.

